Turbulence modulation by small particles in isotropic turbulence

Takeshi Watanabe[†], Izumi Saito and Toshiyuki Gotoh

Department of Physical Science and Engineering,
Nagoya Institute of Technology

1   Introduction

Turbulent flows observed in nature and engineering generally involve the transport of small objects, such as the grains of sand in a river, volcanic ash in the atmosphere, droplets of water or ice crystals in a cloud, or bubbles or polymers in turbulent pipe flow of liquid. Understand the physics of particle-laden turbulent flows is one of the challenging issues of the study of turbulence because the wide range of scales of turbulent motion cause the complicated behavior of particles in space and time. The velocity gradient in turbulence represents highly intermittent fluctuations, leading to anomalous particle diffusion and strong concentrations of particles. Particles in fluids also modify the flow field through momentum coupling, which yields complex interactions between the particles and the carrier fluid. Therefore, many efforts have been made to elucidate the nature of particles in turbulence, not only in terms of the fundamental physics but also for the purpose of developing practical applications [1].

Recent advances in high-performance computing allow us to conduct simulations of particulate flow such that the disturbed flow around each particle is accurately resolved [2]. However, the computational cost of such simulations under realistic conditions is considerably high, even when conducted using state-of-the-art supercomputers. If the particle diameter d is smaller than the smallest size l_K of an eddy in turbulence, it is acceptable to approximate the particle motion by that of a point particle. In computational studies of particulate turbulent flow, the equation of motion of small particles derived by Maxey and Riley [3] has been used to clarify particle statistics, such as binary collisions [4] and preferential concentration [5]. Under point-particle approximation, interactions between an ensemble of particles and turbulence can also be evaluated by a two-way coupling method, in which momentum coupling is evaluated for a Lagrangian point particle and the surrounding computed grid points of the fluid [6]. Turbulence modulation by small solid particles has been extensively investigated by direct numerical simulation (DNS) of turbulence with two-way coupling [7, 8].

One of the important applications of the two-way coupling method for particulate turbulent flows is to clarify polymer-turbulence interactions in which a long-chain polymer is modeled by point particles connected by nonlinear springs [9]. A polymer solution flow shows peculiar flow properties that cannot be observed in a Newtonian fluid. One of the important features of this observation is that a few parts per million of polymer additives can reduce the skin friction of turbulent wall flow by approximately 70%, a phenomenon that is referred to as Tom's effect[10, 11, 12]. This phenomenon is actually applied to the turbulent flows observed in fluid machinery in industry. Another important feature of polymer solution flow is observed in low-Reynolds-number flows, in which the creeping flow becomes unstable and emerges as an unsteady random flow when long-chain polymers are added to the fluid [13]. This phenomenon is referred to as elastic turbulence[14, 15] and has been investigated

from fundamental to applicable viewpoints with the goal of enhancing mixing in micro-fluid devices [16, 17].

There exist the characteristic length and time scales of polymers in flow. The radius of gyration R_g and contour length l_{cntr} for a typical long-chain polymer used in an experimental study of drag reducing flow are approximately $R_g = 0.5 \ \mu m$ and $l_{cntr} \sim l_K$, which is the representative length in turbulence at small scale, called the Kolmogorov length. On the other hand, the typical time scale of a polymer is characterized by the relaxation time τ, which is defined as the time until the extended polymer relaxes to the equilibrium state. Note that τ reaches the order of the eddy turnover time in the inertial range of turbulence, although l_{cntr} is on the order of the smallest representative scale in turbulence.

An important parameter by which to control the polymer-turbulence interactions is the Weissenberg number Wi, which is defined as the ratio of the polymer relaxation time τ to the flow time scale T_{flow}, as $Wi = \tau/T_{flow}$. Polymers are stretched by strong shear in turbulence, but shrink toward an equilibrium state when they are in less turbulent situations. This is the coil-stretch transition [18, 19]. Thus, there exists a critical Weissenberg number at which the polymer configuration drastically changes.

In the present paper, we study turbulence modulation by small particles in isotropic turbulence through large-scale simulations. In particular, we focus on examining polymer-turbulence interactions and polymer scission in isotropic turbulence by performing two-way coupling simulations for polymers (particles) and turbulence (fluid). Polymers are subject to mechanical degradation under intermittent strain-rate fluctuations. Intermittency causes stretching of polymers, leading to polymer scission [20]. As such, the efficiency of polymers as drag-reducing agents diminishes in time. This has a strong impact on industrial applications for the design of drag reducing flow. We herein demonstrate turbulence modulation by polymers [21, 22] and discuss the statistical nature of polymer scission and its effect on the carrier fluid [23].

The remainder of the present paper is organized as follows. In section 2, we present governing equations motion for examining polymer-turbulence interactions by means of two-way coupling simulations. The numerical setup for direct numerical simulations of turbulence and their parameter settings are briefly described in section 3. In section 4, we present the results for the statistical nature of polymer scission and turbulence modulations by polymer additives upon their breakup. Finally, we summarize the results obtained in the present study in section 5.

2 Governing equations of motion

In this section, the governing equations of motion for polymers in turbulence are presented. The motion of a long-chain polymer in fluid is described by the beads-spring model [24]. We consider the dumbbell model, in which the elastic nature of a polymer chain is represented by two beads connected by a nonlinear spring [9]:

$$\frac{d\boldsymbol{R}^{(n)}}{dt} = \boldsymbol{u}_1^{(n)} - \boldsymbol{u}_2^{(n)} - \frac{1}{2\tau^{(n)}} f\left(\frac{|\boldsymbol{R}^{(n)}|}{L_{max}}\right) \boldsymbol{R}^{(n)} + \frac{r_{eq}}{\sqrt{2\tau^{(n)}}}\left(\boldsymbol{W}_1^{(n)} - \boldsymbol{W}_2^{(n)}\right), \qquad (1)$$

$$\frac{d\boldsymbol{r}_g^{(n)}}{dt} = \frac{1}{2}\left(\boldsymbol{u}_1^{(n)} + \boldsymbol{u}_2^{(n)}\right) + \frac{r_{eq}}{\sqrt{8\tau^{(n)}}}\left(\boldsymbol{W}_1^{(n)} + \boldsymbol{W}_2^{(n)}\right), \quad \boldsymbol{u}_\alpha^{(n)} \equiv \boldsymbol{u}(\boldsymbol{x}_\alpha^{(n)}(t), t), \qquad (2)$$

where $\boldsymbol{R}^{(n)}(t)$ and $\boldsymbol{r}_g^{(n)}(t)$ are respectively the end-to-end vector and the center-of-mass vector of the n-th dumbbell. The function $f(z)$ determines the elastic nature of a dumbbell and is expressed by the finitely extensible nonlinear elastic (FENE) model $f(z) = 1/(1 - z^2)$. Here, L_{max} is the maximum extension length of the dumbbell because $f(z \to 1) = \infty$. The term $\boldsymbol{W}_{1,2}^{(n)}(t)$ indicates a random force representing the Brownian motion of particles in the solvent fluid, which obeys Gaussian statistics with a white-in-time correlation of $\langle W_{\alpha,i}^{(n)}(t) \rangle = 0$ and $\langle W_{\alpha,i}^{(m)}(t) W_{\beta,j}^{(n)}(s) \rangle = \delta_{\alpha\beta} \delta_{ij} \delta_{mn} \delta(t - s)$, where $\langle \cdots \rangle$ denotes the ensemble average. The subscripts α, β, i, j, n, and m are assigned values as $(\alpha, \beta) = 1$ and 2; $(i, j) = 1, 2$, and 3; and $(n, m) = 1, 2, \cdots, N_p$. Moreover, δ_{ij} denotes the Kronecker delta. The constant $r_{eq} \equiv \sqrt{k_B T/k}$ is the equilibrium length of the dumbbell under $\boldsymbol{u}(\boldsymbol{x}, t) = \boldsymbol{0}$, where k is the spring constant and k_B and T are the Boltzmann constant and temperature, respectively.

In the present study, the dumbbell is considered to be broken by turbulence if its extension length $R^{(n)}$ exceeds a breakup length l_{sc} even once. This means that polymer scission in turbulence is modeled by means of the relaxation time of n-th polymer $\tau^{(n)}$ as follows:

$$\frac{1}{\tau^{(n)}} = \begin{cases} \tau^{-1} & t < t_{sc}^{(n)} \\ 0 & t \geq t_{sc}^{(n)} \end{cases} \tag{3}$$

where $\tau \equiv \zeta/4k$ and $t_{sc}^{(n)}$ is the smallest time such that $R^{(n)} = l_{sc}$.

The turbulent velocity field acts as an incompressible fluid and the Navier-Stokes (NS) equations

$$\nabla \cdot \boldsymbol{u} = 0, \qquad \frac{\partial \boldsymbol{u}}{\partial t} + \boldsymbol{u} \cdot \nabla \boldsymbol{u} = -\nabla p + \nu_f \nabla^2 \boldsymbol{u} + \nabla \cdot \boldsymbol{T}^p. \tag{4}$$

Here, ρ_f is set to unity and equals the density of bead ρ_p. In addition, $\boldsymbol{T}^p(\boldsymbol{x}, t)$ is the polymer stress tensor due to the force acting on the fluid from the dispersed dumbbells, defined by

$$T_{ij}^p(\boldsymbol{x}, t) = \frac{\nu_f \eta L_{box}^3}{N_p(0)} \sum_{n=1}^{N_p(0)} \frac{1}{\tau^{(n)}} \left[\frac{R_i^{(n)} R_j^{(n)}}{r_{eq}^2} f\left(\frac{|\boldsymbol{R}^{(n)}|}{L_{max}} \right) - \delta_{ij} \right] \delta(\boldsymbol{x} - \boldsymbol{r}_g^{(n)}), \tag{5}$$

where $N_p(0)$ is the total number of dumbbells at $t = 0$ used in our simulations. In addition, L_{box} is the linear size of the domain, and η is the ratio of the zero-shear viscosity ν_p of the polymer to the solution viscosity ν_f ($\eta = \nu_p/\nu_f$). Note that η is proportional to the volume fraction of dumbbells Φ_V by $\eta \equiv (3r_{eq}/4a)^2 \Phi_V$. Moreover, $1/\tau^{(n)}$ in eq. (5) means that the dumbbells stop affecting the turbulent velocity field after their breakup.

3   Setup for numerical simulations

The two-way coupling simulations of eqs. (1) through (5) are performed in a periodic box with periodicity $L_{box} = 2\pi$ using the pseudo-spectral method in space and the second-order Runge–Kutta method in time. A total of 128^3 grid points are set to solve the NS equations. The statistically isotropic turbulence is accomplished by imposing linear external forcing $\hat{\boldsymbol{f}}_{ext}(k, t) = A(t)\hat{\boldsymbol{u}}(\boldsymbol{k}, t)$ within the wavenumber shell $1 \leq |\boldsymbol{k}| \leq 2$ and is zero otherwise, and the amplitude $A(t)$ is determined by maintaining the energy input rate ε_{in} to be constant in time. We set $\varepsilon_{in} = 0.5$ and $\nu = 0.015$, which yields the Taylor-microscale Reynolds number $Re_\lambda = 51$ in the case of one-way coupling.

The number of dumbbells $N_p(0) = 4 \times 10^8$ is dispersed into the fluid with $\eta = 4 \times 10^{-2}$ after the statistically steady turbulence is obtained. The time at which the dumbbells are dispersed into the flow is $t = 0$. The maximum extension length and critical scission length are respectively set as $L_{max} = \sqrt{9000}r_{eq}$ and $l_{sc} = 0.8L_{max}$. The dumbbells are uniformly and randomly distributed over the computational domain. The initial configuration of each dumbbell is set according to $\boldsymbol{R}^{(m)}(0) = \sqrt{3}r_{eq}\boldsymbol{n}^{(m)}$, where $\boldsymbol{n}^{(m)}$ is a unit vector, the orientation of which is randomly distributed. Three cases of the Weissenberg number $Wi = 0.6, 0.8$, and 1.0, which is the non-dimensional polymer relaxation time $\lambda\tau$ defined using the Lyapunov exponent of the Newtonian turbulent flow, are considered for the cases of one-way and two-way coupling simulations.

The fluid velocity at the bead positions $\boldsymbol{u}(\boldsymbol{x}_\alpha^{(n)})$ is evaluated using the tri-linear interpolation scheme, whereas the delta function appeared in the polymer stress term (5) is approximated by the weight function

$$\delta_\Delta(\boldsymbol{x} - \boldsymbol{r}_g^{(n)}) = d_\Delta(x_1 - r_{g,1}^{(n)})d_\Delta(x_2 - r_{g,2}^{(n)})d_\Delta(x_3 - r_{g,3}^{(n)}), \tag{6}$$

with

$$d_\Delta(x) = \begin{cases} \frac{1}{\Delta}\left(1 - \frac{|x|}{\Delta}\right) & (|x| \leq \Delta) \\ 0 & (|x| > \Delta) \end{cases} \tag{7}$$

where Δ was chosen based on the grid spacing Δx [6]. The weight given by (7) is the same as that used in the tri-linear interpolation for evaluating $\boldsymbol{u}(\boldsymbol{x}_\alpha^{(n)})$. The computation is performed using parallelized code written by Message Passing Interface (MPI) and Open MP. For more details on parallel computation, please refer to the reference [25].

4 Results and discussions

4.1 Polymer scission statistics in isotropic turbulence

Temporal decays of the fraction of unbroken dumbbells $N_p(t)/N_p(0)$ obtained by one-way (passive polymer, thin lines) and two-way (active polymer, thick lines) coupling simulations are shown in figure 1. In the case for one-way coupling, the decay is exponential $\exp(-t/T_d)$ with a time scale T_d, as seen in the theoretical prediction [23]. Moreover, T_d also decreases with increasing Wi, being in agreement with the theory [23]. In the cases for two-way coupling, on the other hand, the scission process is composed of two stages: (i) an early-time regime in which the dumbbells break up much slower than in the case of one-way coupling and (ii) a long-time regime in which the active dumbbells show the exponential decay, just like passive dumbbells. In the early-time regime (i), the fraction of unbroken dumbbells decays as $1 - k(t - t^*)$ with $t^*/\tau_\eta = 23$ and $k\tau_\eta \times 10^3 = 0.315, 1.10$, and 2.41 for $Wi = 0.6, 0.8$, and 1.0, respectively, as presented in figure 1(b). Thus, the decay rate k increases with Wi, indicating that the onset of the exponential decay regime is hastened with increasing Wi.

Figure 2 shows the time-integrated probability density function (p.d.f.) of the end-to-end distance $R = |\boldsymbol{R}^{(n)}|$ of unbroken dumbbells for (a) $Wi = 0.8$ and (b) $Wi = 1.0$, respectively. The p.d.f. clearly displays a power-law form $P(R) \sim R^2$ for $R \ll \sqrt{3}r_{eq}$ for both cases of one-way and two-way coupling simulations. This originates from the fact that
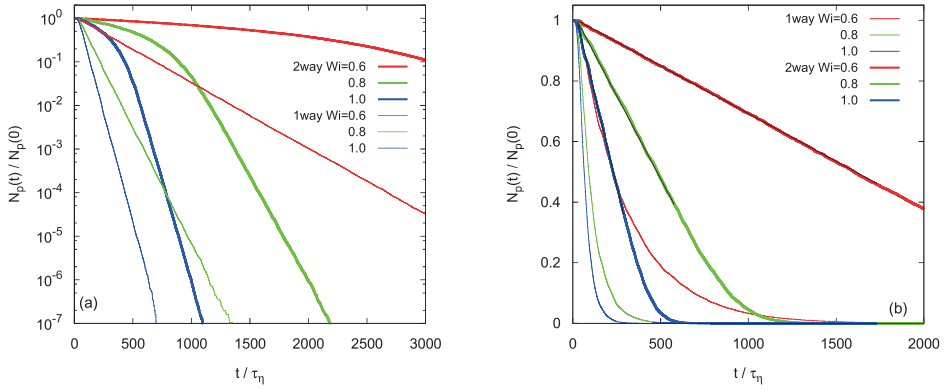
Figure 1: Temporal evolution for the fraction of unbroken dumbbells $N_p(t)/N_p(0)$ as a function of non-dimensional time t/τ_η using Kolmogorov time τ_η: (a) plotted on a semilogarithmic scale and (b) plotted on a linear scale. Thin curves show the results obtained for one-way coupling cases.

the dumbbell dynamics is dominated by thermal agitation, being independent of the nature of turbulent flows and the value of Wi. On the other hand, the right-hand tail of the p.d.f., $R \gg \sqrt{3}r_{eq}$, shows power-law decay similar to R^{-1}, which is theoretically predicted by the case of $Wi > Wi_{cr}$. Note that $Wi_{cr} = 1/2$ is the value whereby the ensemble of dumbbells indicates the coil-stretch transition [19]. In the range $R \gg \sqrt{3}r_{eq}$, it is theoretically shown that $P(R) \sim R^{-1-\alpha}$ with $\alpha = 3(Wi^{-1} - 2)/2$ when $Wi < Wi_{cr}$ or $P(R) \sim R^{-1}$ when $Wi > Wi_{cr}$ [23]. For the curves obtained by two-way coupling simulations, on the other hand, the power-law decay cannot be observed in the range $R \gg \sqrt{3}r_{eq}$ (blue lines) as the one-way coupling. This observation is attributed to the turbulence modulations by unbroken dumbbells, as described in a later section.

The effect of active polymer feedback on turbulence can also be seen in the p.d.f. of the lifetime of dumbbells $P(T_{sc})$, as shown in figure 3, in which the p.d.f.s are evaluated for the (a) one-way and for (b) two-way coupling cases, respectively. Here, T_{sc} is the first passage time when the dumbbell extension length $R^{(n)}$ exceeds l_{sc}. In the case of one-way coupling (passive dumbbells), $P(T_{sc})$ decays exponentially, and its decay rate increases with increasing Wi. In fact, $P(T_{sc})$ is related to the number density of unbroken dumbbells by $1 - N_p(t)/N_p(0) = \int_0^t P(T_{sc}) \, dT_{sc}$, representing that the decay rate of $P(T_{sc})$ is same as that of $N_p(t)$. Whereas, in the case of two-way coupling (active dumbbells), we can observe a plateau in the smaller T_{sc} range, which corresponds to the early-time regime found in figure 1. This behavior is also consistent with the observation of decay law $1 - k(t - t^*)$ in figure 1(b). The amplitude of $P(T_{sc})$ in this plateau is evaluated by $k\tau_\eta \times 10^3 = 0.315, 1.10$, and 2.41 for $Wi = 0.6, 0.8$, and 1.0, respectively. In the long-time regime, on the other hand, $P(T_{sc})$ exhibits the same exponential decay as $N_p(t)$ in figure 1(a) and in the one-way coupling case of $P(T_{sc})$ in figure 3(a).
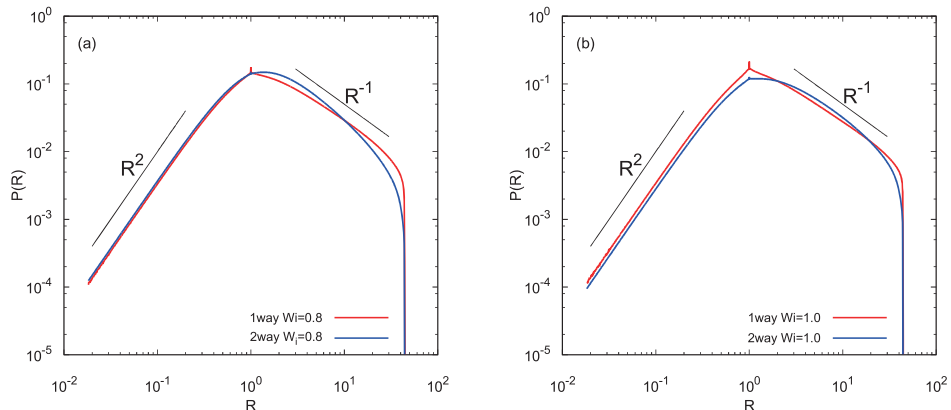
Figure 2: Time integrated p.d.f. of the end-to-end distance of unbroken dumbbells in the cases for (a) $Wi = 0.8$ and (b) $Wi = 1.0$, respectively. Red (blue) curve shows the result obtained for one-way (two-way) coupling cases.

4.2 Effect of polymer scission on turbulence statistics

The kinetic energy of fluid motion $E(t)$ and the elastic energy of the ensemble of dumbbells $U(t)$ are respectively defined as follows:

$$E(t) = \frac{1}{2}\langle |\boldsymbol{u}|^2 \rangle_V, \tag{8}$$

$$U(t) = -\left(\frac{L_{max}}{r_{eq}}\right)^2 \frac{\nu\eta}{N_p(0)} \sum_{m=1}^{N_p(0)} \frac{1}{2\tau^{(m)}} \ln\left[1 - \left(\frac{|\boldsymbol{R}^{(m)}(t)|}{L_{max}}\right)^2\right]. \tag{9}$$

Temporal evolution for $E(t)$ and $U(t)$ are then governed by the following equations:

$$\frac{dE}{dt} = -\varepsilon(t) - \varepsilon_p(t) + \varepsilon_{in}, \tag{10}$$

$$\frac{d}{dt}U(t) = \varepsilon_p'(t) - \varepsilon_S(t) + \varepsilon_B(t). \tag{11}$$

The term $\varepsilon_p(t)$ in the right-hand side of eq. (8) represents the polymer effects on the kinetic energy variation and is defined by

$$\varepsilon_p(t) = \langle \partial_i u_j T_{ij}^p \rangle_V = \langle S_{ij} T_{ij}^p \rangle_V, \tag{12}$$

where $S_{ij} = (\partial_i u_j + \partial_j u_i)/2$. This term originates from the polymer stress field added to the NS equations and contributes to the energy exchange between the turbulence and the ensemble of dumbbells. Here, $\varepsilon(t) = \nu \langle (\nabla \boldsymbol{u})^2 \rangle_V$ and ε_{in} are respectively the mean kinetic energy dissipation rate due to the viscosity of fluid and the energy input rate originated from the external forcing. The term $\varepsilon_p'(t)$ is defined by

$$\varepsilon_p'(t) = \frac{\nu\eta}{r_{eq}^2} \frac{1}{N_p(0)} \sum_{m=1}^{N_p(0)} \frac{1}{\tau^{(m)}} \left(u_\alpha(\boldsymbol{x}_1^{(m)}) - u_\alpha(\boldsymbol{x}_2^{(m)})\right) R_\alpha^{(m)} f\left(\frac{|\boldsymbol{R}^{(m)}|}{L_{max}}\right). \tag{13}$$
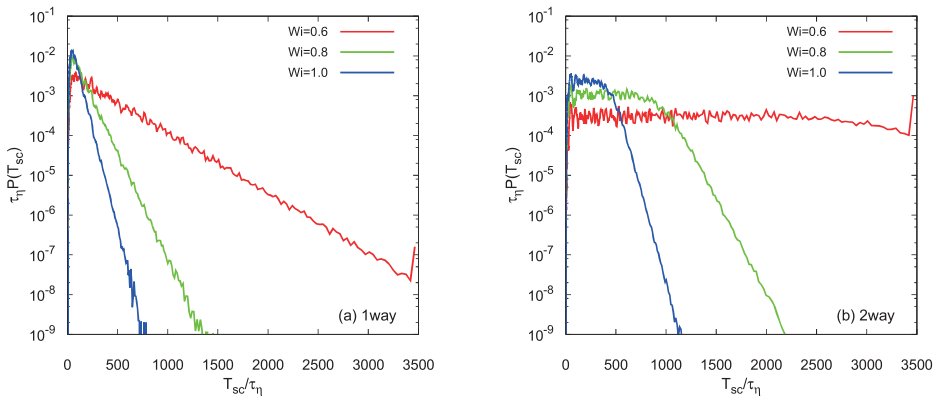
Figure 3: Probability density function for the lifetime of dumbbells for $Wi = 0.6$ (red), $Wi = 0.8$ (green) and $Wi = 1.0$ (blue) obtained by (a) one-way coupling and (b) two-way coupling simulations, respectively.

Note that $\varepsilon_p'(t)$ equals $\varepsilon_p(t)$ (12) because of Newton's third law. If $\varepsilon_p'(t) > 0$, then the dumbbells absorb kinetic energy from the turbulent fluid motion, while for $\varepsilon_p'(t) < 0$, the elastic energy stored in the ensemble of dumbbells is released and transferred to the fluid. If the fluid motion plays only a minor part in the dumbbell dynamics, then, as is the case for $Wi \ll 1$, we expect that $\varepsilon_p'(t) \simeq 0$. In this case, the dumbbells remain in a thermal equilibrium state. The terms ε_S and ε_B are the work performed by the elastic force and the work performed by the thermal agitation, respectively [21]. The term $\varepsilon_S(t)$ acts to suppress the increase in elastic energy due to the elastic force among the beads, and $\varepsilon_S(t) > 0$.

Figure 4 shows the temporal evolution of both the mean kinetic energy $E(t)$ of turbulent fluid and the elastic energy $U(t)$ evaluated by the ensemble of dumbbells for the two-way coupling simulations. In the early-time regime observed in figures 1 and 3, $E(t)$ rapidly decreases with time and then gradually increases up to the level of the initial state of turbulence. This feature is clearly seen for $Wi = 1.0$ when compared to the case of $Wi = 0.6$. This is due to the fact that the higher $Wi(> Wi_{cr})$ dumbbells are more greatly stretched by turbulence, leading to both the stronger impact on the decreasing turbulence intensity of fluctuation and obtaining several chances to exceed the breakup length l_{sc}. Therefore, $E(t)$ is gradually increased with time once the number of broken dumbbells increases. This can also be recognized in the behavior of $U(t)$ in figure 4(b), where $U(t)$ increases for $t < 100\tau_\eta$ due to the increase in the number of stretched dumbbells, whereas $U(t)$ decreases with time as the number of surviving dumbbells decreases.

The temporal evolutions of (a) $\varepsilon(t)$ and (b) $\varepsilon_p(t)$ obtained for the case of two-way coupling simulations are shown in figure 5. Note that $\varepsilon_{in} = \overline{\varepsilon} + \overline{\varepsilon_p}$ under the statistically steady state. The feedback force on turbulence by dumbbells is fairly strong at short times ($t < 100\tau_\eta$), leading to a significant reduction in kinetic energy dissipation ε and the amplification of energy transfer to the ensemble of dumbbells ($\varepsilon_p(t)$). Reduction of $\varepsilon(t)$ means that the amplitude of the rate of strain S_{ij} is also decreased, yielding weaker stretching of dumbbells
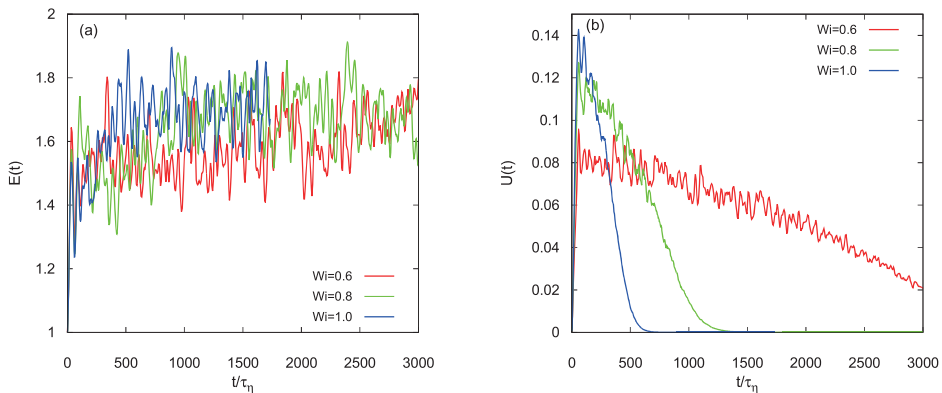
Figure 4: Temporal evolution for (a) the volume-averaged kinetic energy of fluid $E(t)$ and (b) the elastic energy of the ensemble of dumbbells obtained by the two-way coupling simulations.

and a lower probability of their scission, as observed in the early-time regime of figure 1. However, the concentration of unbroken dumbbells continues to decrease until the feedback force on turbulence becomes negligibly small. Then, $\varepsilon(t)$ returns to the value expected in the case of Newtonian fluid turbulence, and $\varepsilon_p(t)$ becomes zero. In this later regime, active dumbbells are broken by turbulence under a similar condition to one-way coupling calculations, resulting in exponential decays of both $N_p(t)$ and $P(T_{sc})$ obtained by two-way coupling simulations that are similar to those obtained for the one-way coupling case. Dumbbells break more easily for higher Wi values, indicating that the time needed for the feedback force to vanish decreases with increase of Wi, as shown in figure 5. In the case of $Wi = 0.6$, breakup events proceed slowly and the reduction of energy dissipation lasts for a longer time.

5 Conclusion

In the present paper, we have examined the statistical nature of polymer scission in turbulence and its effect on turbulence modulation by performing Eulerian-Lagrangian simulations for the ensemble of dumbbells (particle-based polymer model) dispersed in steady isotropic turbulence. The concentration of unbroken dumbbells was found to decay exponentially in time when the feedback force from the ensemble of dumbbells is neglected (one-way coupling case). On the other hand, for the two-way coupling simulations in which the feedback force of dumbbells is considered, we found that the temporal decay of $N_p(t)$ is characterized by the two kinds of regime (early-time and long-time regimes). We found that a long-time regime shows exponential decay, the decay rate of which is close to that obtained by one-way coupling. In an early-time regime, on the other hand, it was shown that $N_p(t)$ decays linearly as $N_p(t)/N_p(0) = 1 - k(t - t^*)$. The decay law in an early-time regime could also be clarified in the behavior of the lifetime p.d.f. of dumbbells in the shorter time range. Modification of
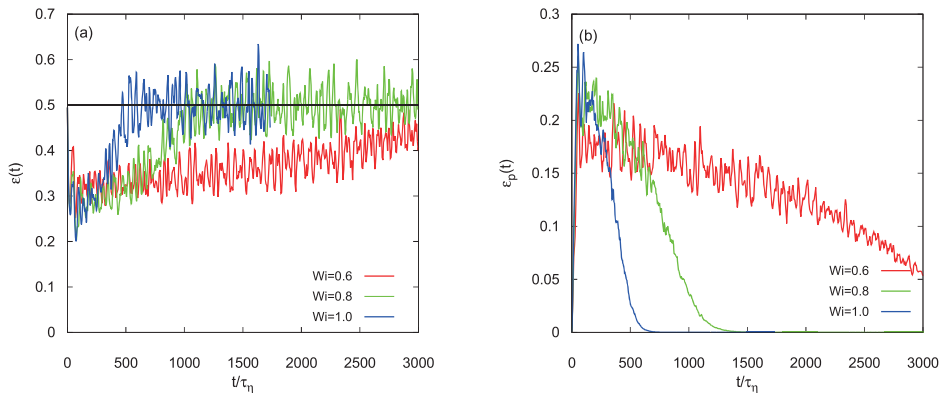
Figure 5: Temporal evolution for (a) the mean dissipation rate of the kinetic energy of fluid $\varepsilon(t)$ and (b) the rate of energy exchange between the ensemble of dumbbells and turbulent fluid $\varepsilon_p(t)$ obtained by the two-way coupling simulations.

scission statistics of dumbbells by two-way coupling was found in the right-hand tail of the time-integrated p.d.f. for extension length $R^{(n)}$ of dumbbells, where we could not observe power law decay such as $P(R) \sim R^{-1}$, which is predicted by the theory and by the one-way coupling simulations.

Turbulence modulation was also examined by investigating fundamental statistical quantities appearing in the evolution equations for the kinetic energy of turbulent fluid and the elastic energy of the ensemble of dumbbells. The volume-averaged kinetic energy decreased with time in the shorter time range and then returned to the turbulent state of the Newtonian fluid in the later time range. The elastic energy of the ensemble of dumbbells, on the other hand, increased with time in the shorter time range due to the stretching of dumbbells. However, in the later time range, dumbbells were easily broken by turbulence, which leads to the decrease in both $U(t)$ and the feedback force. This feature was also clarified in the behavior of the mean dissipation rate of kinetic energy and the rate of energy exchange between the ensemble of dumbbells and turbulent fluid. Reduction of $\varepsilon(t)$ caused by stretching dumbbells became larger for larger Wi in a shorter time, and the value of $\varepsilon(t)$ gradually returned to that obtained by Newtonian fluid turbulence.

Acknowledgements

References

[1] G. Falkovich, K. Gawedzki and M. Vergasola, "Particles and fields in fluid turbulence",Rev. Mod. Phys. **73**, 913 (2001).

[2] M. Uhlmann, "An immersed boundary method with direct forcing for the simulation of particulate flows", J. Comput. Phys. **209**, 448 (2005).

[3] M. R. Maxey and J. J. Riley, "Equation of motion for a small rigid sphere in a nonuniform flow", Phys. Fluids 26, **883** (1983).

[4] S. Sundaram and L. R. Collins, "Collision statistics in an isotropic particle-laden turbulent suspension. Part 1. Direct numerical simulations",J. Fluid Mech. **335**, 75 (1997).

[5] K. D. Squires and J. K. Eaton, "Preferential concentration of particles by turbulence",Phys. Fluids A: Fluid Dynamics **3**, 1169 (1991).

[6] A. Prosperetti and G. Tryggvasson, "Computational Methods for Multiphase Flow" (ed. A. Prosperetti and G. Tryggvason), Cambridge University Press (2007).

[7] A. Ferrante and S. Elghobashi, "On the physical mechanisms of two-way coupling in particle-laden isotropic turbulence",Phys. Fluids 15, **315** (2003).

[8] I. Saito, T. Watanabe and T. Gotoh, "A new time scale for turbulence modulation by particles", J. Fluid Mech. **880**, R6 (2019).

[9] R. B. Bird, C. F. Curtiss, R. C. Amstrong, and O. Hassager, *"Dynamics of Polymetric Liquids, Vol.2 Kinetic Theory"*, 2nd ed. (Wiley, New York, 1987).

[10] J. L. Lumley, "Drag Reduction in Turbulent Flow by Polymer Additives", *J. Polymer Sci.: Macromolecular Reviews* **7**, 263–290 (1973).

[11] K. R. Sreenivasan and C. M. White, "The onset of drag reduction by dilute polymer additives, and the maximum drag reduction asymptote", *J. Fluid Mech.* **409**, 149–164 (2000).

[12] I. Proccaccia, V. S. L'vov, and R. Benzi, "Theory of drag reduction by polymers in wall-bounded turbulence", *Rev. Mod. Phys. 80*, 225 (2008).

[13] R. G. Larson, Eric S. G. Shaqfeh, and S. J. Muller, "A purely elastic instability in Taylor-Couette flow", J. Fluid Mech. **218**, 573–600 (1990).

[14] A. Groisman and V. Steinberg, "Elastic turbulence in a polymer solution flow", *Nature* **405**, 53–55, (2000).

[15] A. Groisman and V. Steinberg, "Elastic turbulence in curvilinear flows of polymer solutions", *New J. Phys.*, **6**, 29 (2004).

[16] A. Groisman and V. Steinberg, "Efficient mixing at low Reynolds numbers using polymer additives", *Nature* **410**, 905–908, (2001).

[17] P. E. Arratia, C. C. Thomas, J. Diorio, and J. P. Gollub, "Elastic Instabilities of Polymer Solutions in Cross-Channel Flow", *Phys. Rev. Lett.* **96**, 144502 (2006).

[18] P. G. De Gennes, "Coil-stretch transition of dilute flexible polymers under ultrahigh velocity gradients", *J. Chem. Phys.* **60**, 5030–5042 (1974).

[19] T. Watanabe and T. Gotoh, "Coil-stretch transition in an ensemble of polymers in isotropic turbulence", Phys. Rev. E **81**, 066301 (2010).

[20] E. J. Soares, "Review of mechanical degradation and de-aggregation of drag reducing polymers in turbulent flow", J. Non-Newtonian Fluid Mech. **276**, 104225 (2020).

[21] T. Watanabe and T. Gotoh, "Hybrid Eulerian-Lagrangian simulations for polymer-turbulence interactions", J. Fluid Mech. **717**, 535 (2013).

[22] T. Watanabe and T. Gotoh, "Power-law spectra formed by stretching polymers in decaying isotropic turbulence", *Phys. Fluids* **26**, 035110 (2014).

[23] D. Vincenzi, T. Watanabe, S. S. Ray and J. R. Picardo, "Polymer scission in turbulent flows", J. Fluid Mech. **912**, A18 (2020).

[24] M. Doi and S. F. Edwards, "*The Theory of Polymer Dynamics*", (Oxford University Press, New York, 1986).

[25] T. Watanabe and T. Gotoh, " Kinetic energy spectrum of low-Reynolds-number turbulence with polymer additives", *J. Phys.: Conf. Ser.* **454**, 012007 (2013).

Department of Physical Science and Engineering
Nagoya Institute of Technology
Gokiso, Showa-ku, Nagoya 466-8555
JAPAN
E-mail address: [†]watanabe@nitech.ac.jp